Supporting Information

Schoebel et al. 10.1073/pnas.1113133108

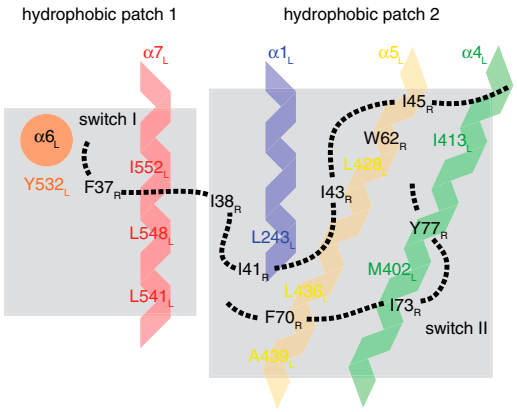

Fig. S1. Hydrophobic patches in LidA. Four α-helices ($\alpha 1_L$, $\alpha 4_L$, $\alpha 5_L$, and $\alpha 7_L$) of LidA provide a platform for the binding of Rab8a. Hydrophobic residues in the switch regions of Rab8a (dotted lines with indicated amino acids) bind to two hydrophobic patches (patch I and II) on the LidA helices.

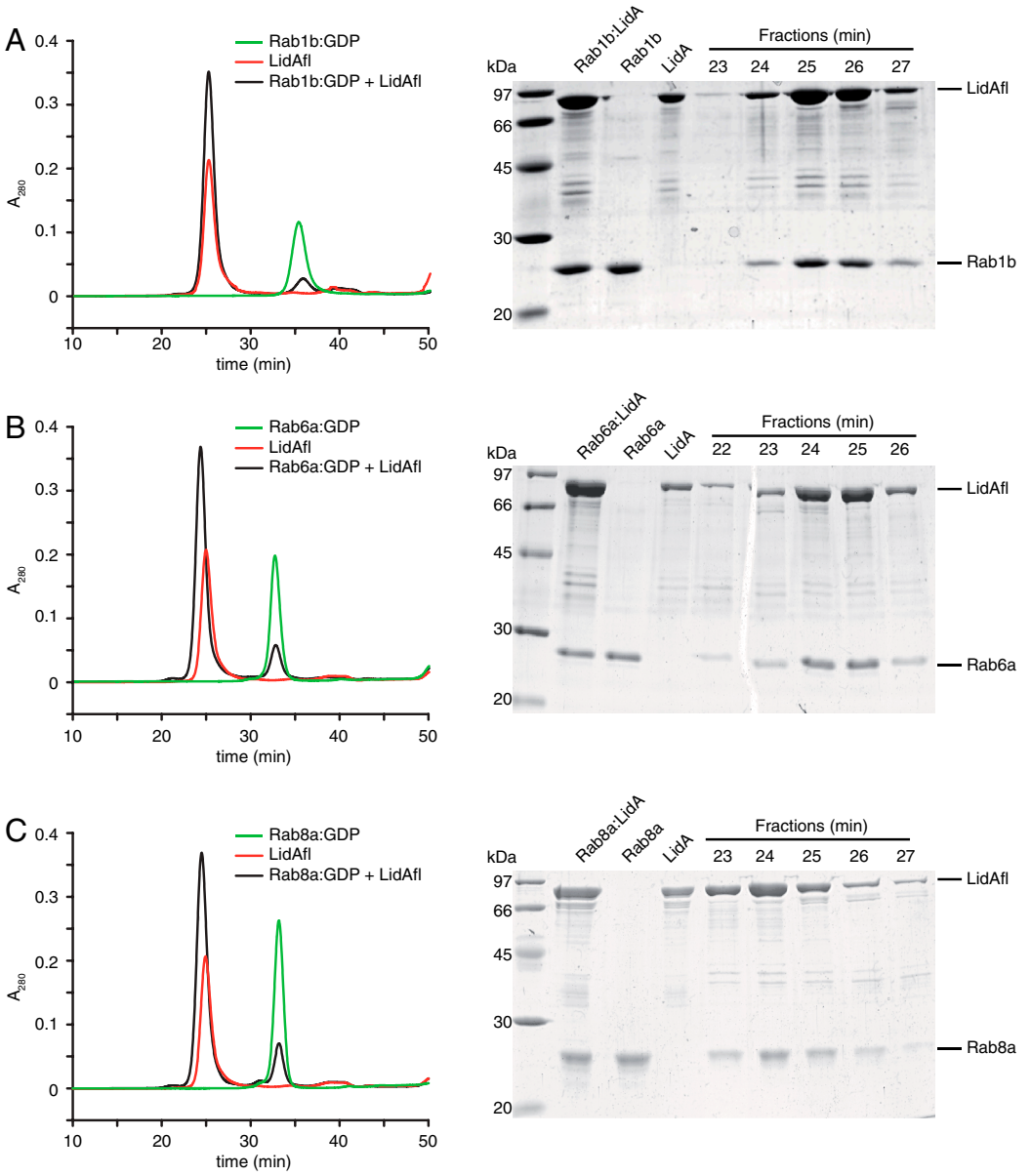

Fig. S2. Complex formation of Rab1b, Rab6a, and Rab8a with LidA, analyzed by size exclusion chromatography. Complex formation of Rab1b (*A*), Rab6a (*B*), and Rab8a (*C*) with full-length LidA was analyzed on a Superdex 200 10/30 column (GE Healthcare) by monitoring the UV absorption at 280 nm (*Left*). Complex fractions were subjected to denaturing polyacrylamide gel electrophoresis (SDS-PAGE) to verify Rab and LidA coelution (*Right*). An amount of 400 μg LidA and 150 μg Rab were applied per gel filtration run.

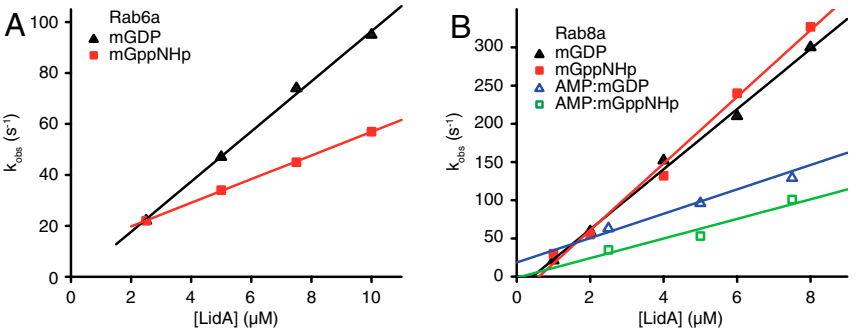

Fig. S3. Association kinetics of Rab6a and Rab8a with $LidA_{201–583}$. The time-dependent association of 1 μM Rab6a (*A*) or Rab8a (*B*) with $LidA_{201–583}$ was analyzed by stopped-flow monitoring the change in fluorescence polarization. The fluorescence polarization time traces were fitted to single exponentials, and the observed rate constants for association were plotted against the $LidA_{201–583}$ concentration. From the slope of the linear regression, the association rate constants (k_{on}) are obtained.

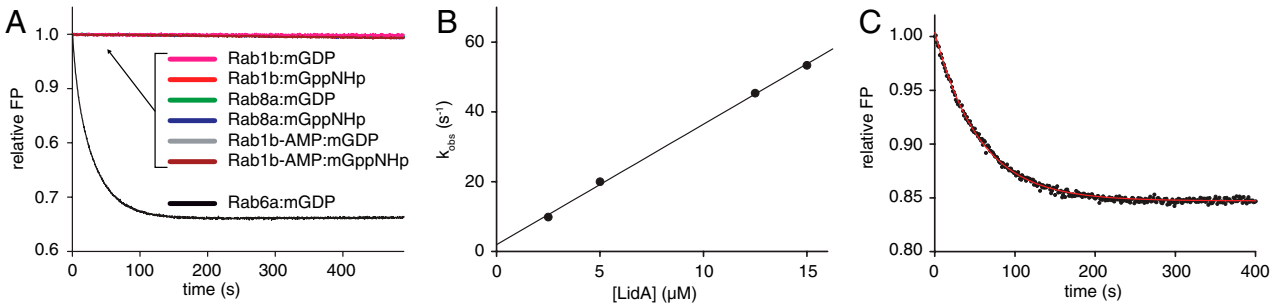

Fig. S4. Interaction of fluorescent Rab proteins with LidA. (*A*) Displacement of fluorescent Rab proteins from LidA. Prior to the experiment $LidA_{201–583}$ was bound to different fluorescent Rab proteins (in the mGDP or mGppNHp state, either adenylylated or nonadenylylated) as indicated. A concentration of 1.0 μM of each complex was shot against a 10× excess of nonfluorescent Rab protein to follow the time-dependent dissociation of the fluorescent Rabs by fluorescence polarization (FP). The displacement of Rab6a:mGDP from LidA is shown as a positive control. However, Rab1b and Rab8a could not be displaced from LidA. (*B*) Determination of the association rate constant (k_{on}) for Rab6:mGDP interaction with full-length LidA ($LidA_{fl}$). The slope of a linear fit of the observed rate constants (k_{obs}) in dependence on the $LidA_{fl}$) concentration gives $k_{on} = 3.5\,10^6\ M^{-1}\,s^{-1}$. The k_{obs} values have been obtained from fitting the change in fluorescence polarization upon shooting 1 μM Rab1b against increasing concentrations of $LidA_{fl}$ to a single exponential. (*C*) Displacement of 0.2 μM Rab6a:mGDP from $LidA_{fl}$ by nonfluorescent Rab1b:GppNHp (2 μM) monitored by FP, fitted to a single exponential (red line) ($k_{off} = 0.018\ s^{-1}$).

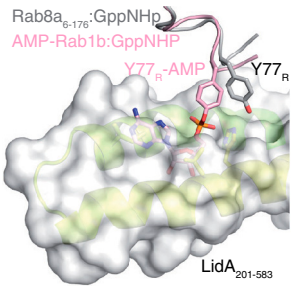

Fig. S5. Rab1b-AMP cannot bind to LidA in an identical manner to Rab8a as seen in the $Rab8a_{6–176}$:$LidA_{201–583}$ complex structure. The position of $Y77_R$ of Rab8a demonstrates that an AMP group on the Rab protein would clash with LidA surface when bound in the same mode in which the nonadenylylated Rab8 binds to LidA. The position of the AMP group is inferred from a superimposition Rab1b-AMP (Protein Data Bank ID code 3NKV) with Rab8a from the $Rab8a_{6–176}$:$LidA_{201–583}$ complex structure.

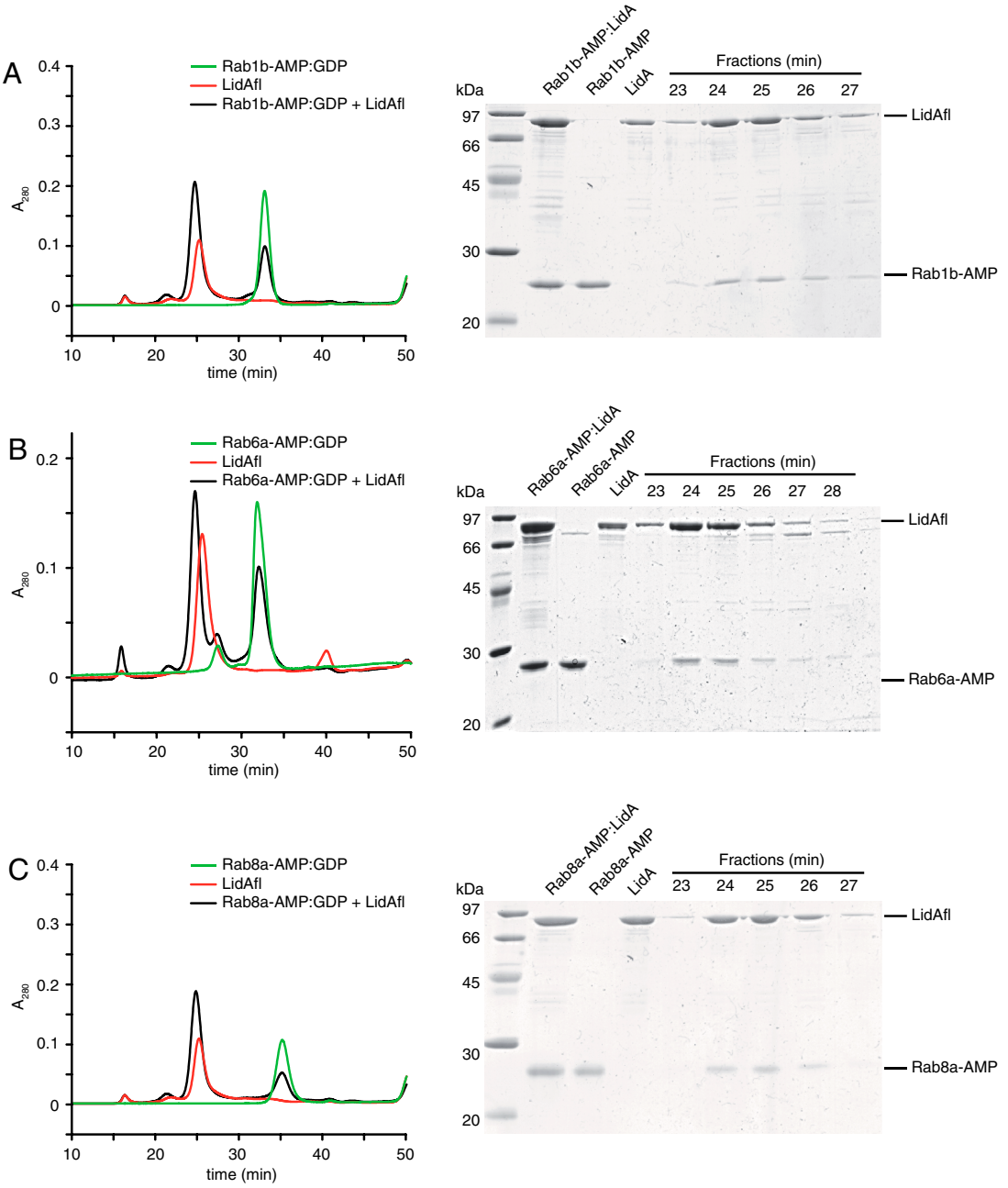

Fig. S6. Complex formation of adenylylated Rab1b, Rab6a, and adenylylated Rab8a with LidA, analyzed by size exclusion chromatography. Complex formation of Rab1b-AMP (*A*), Rab6a (*B*), and Rab8a-AMP (*C*) with full-length LidA was analyzed on a Superdex 200 10/30 column (GE Healthcare) by monitoring the UV absorption at 280 nm (*Left*). Complex fractions were subjected to denaturing polyacrylamide gel electrophoresis (SDS-PAGE) to verify Rab and LidA coelution (*Right*). An amount of 400 μg LidA and 150 μg Rab were applied per gel filtration run.

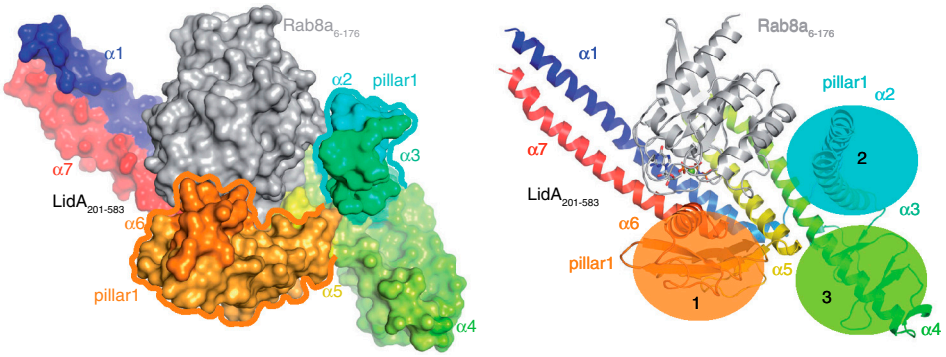

Fig. S7. The structure of LidA reveals potential binding sites of other binding partners. Surface representation (*Left*) and cartoon model (*Right*) of the $Rab8a_{6–176}$: $LidA_{201–583}$ complex structure. Three regions [1–3, colored circles (*Right*)] opposite to the bound Rab (gray) suggest that other (unknown) factors could interact with the Rab-LidA complex. Because the affinity between LidA and Rab1b or Rab8a is unusually high (K_d pM-nM), the need for a factor acting on LidA in order to displace the tightly bound Rab is conceivable. Such displacement factor binding site would probably have to be spatially distant from the Rab-binding site of LidA, as would be the case for regions 1–3. Because pillar II of LidA establishes multiple contacts to Rab8a, an interaction of a third factor with this pillar from the site opposite to Rab8 could significantly modulate the Rab affinity.

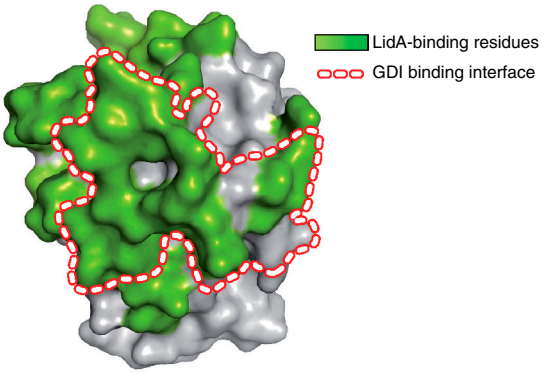

Fig. S8. The binding sites of LidA and GDP dissociation inhibitor (GDI) on Rab proteins overlap. The figure depicts Rab8a from the Rab8a : LidA complex structure in surface representation. Surface residues colored in green are interacting with LidA. The line dotted in white and red encircles the interface with GDI (inferred from homology considerations with the Ypt1 : GDI complex). Because the binding sites of LidA and GDI overlap greatly, a ternary complex among Rab, LidA, and GDI will not be possible.

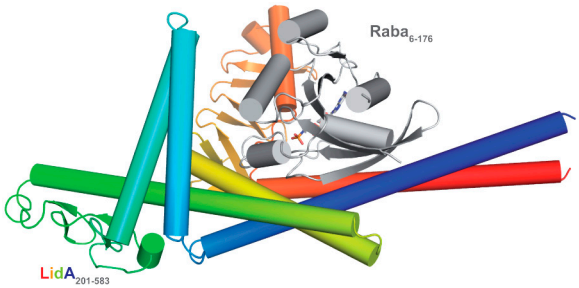

Movie S1 Movie of the $Rab8a_{6–176}$: $LidA_{201–583}$ complex. Rab8a is shown in gray, LidA from blue (N terminus) to red (C terminus), and GppNHp is shown in stick representation. The α-helices are shown as cylinders. Coloring and depiction of secondary structure elements are according to Fig. 1*A*.

Movie S1 (MOV)

Table S1. Data collection and refinement statistics for Rab8a$_{6–176}$:LidA$_{201–583}$

	Se-SAD* LidA$_{201–583}$:Rab8$_{6–176}$	LidA$_{201–583}$:Rab8$_{6–176}$
Data collection†		
Space group	$P4_32_12$	$P4_32_12$
Cell dimensions		
A, *B*, *C*, Å	103.33, 103.33, 150.33	103.82, 103.82, 150.61
α, β, γ, °	90, 90, 90	90, 90, 90
Wavelength, Å	0.9786	0.9786
Resolution, Å	30–3.2	30–2.5
R_{merge}‡	2.9 (10.7)	5.2 (39.7)
$I/\sigma(I)$	44.36 (14.63)	26.34 (4.59)
Completeness, %	100 (100)	99.8 (99.5)
Redundancy	72.1 (76)	10.7 (11.2)
Refinement		
No. reflections		312,773 (29,145)
R_{work}		21.6
R_{free}		27.5
No. atoms		
Protein		4458
Ligand/ion		81
Water		48
B factors		
Protein		72
Ligand/Ion		60
Water		53.7
rms deviation		
Bond length, Å		0.009
Bond angle, °		1.114
PDB ID code		3TNF

Values in parentheses refer to the highest resolution shell.

*Data collection statistics for single-wavelength anomalous dispersion data refer to unmerged Friedel pairs.

†The dataset was collected from one single crystal on beamline X10SA of the Swiss Light Source (Paul Scherrer Institute).

‡Calculated as defined by Diederichs and Karplus (1).

1. Diederichs K, Karplus PA (1997) Improved R-factors for diffraction data analysis in macromolecular crystallography. *Nat Struct Biol* 4:269–275.